Classification of EEG Spectrogram Image with ANN approach for Brainwave Balancing Application

Mahfuzah Mustafa[1,2]
[1]Faculty of Electrical & Electronics
Universiti Malaysia Pahang
26600 Pekan, Pahang, Malaysia
mahfuzah@ump.edu.my

Mohd Nasir Taib[2], Zunairah Hj Murat[2],
Norizam Sulaiman[1,2], Siti Armiza Mohd Aris[2]
[2]Faculty of Electrical Engineering
Universiti Teknologi MARA
40450, Shah Alam, Selangor, Malaysia
dr.nasir@ieee.org

***Abstract*—In this paper, an Artificial Neural Network (ANN) algorithm for classifying the EEG spectrogram images in brainwave is presented. Gray Level Co-occurrence Matrix (GLCM) texture feature from the EEG spectrogram images have been used as input to the system. The GLCM texture feature produced large dimension of feature, therefore the Principal Component Analysis (PCA) is used to reduce the feature dimension. The result shows that the proposed model is able to classify EEG spectrogram images with 77% to 84% accuracy for three classes of brainwave balancing application with an optimized ANN model in training by varying the neurons in the hidden layer, epoch, momentum rate and learning rate.**

Keywords – EEG, spectrogram image, GLCM, PCA, ANN

I. INTRODUCTION

Artificial neural network (ANN) is inspired from the human brain by mimicking the action of neurons in the brain. ANN is a popular and powerful algorithm in data mining. The best performance can be achieved by varying the weights during training process. The feed forward training algorithm is normally used for the ANN in Electroencephalogram (EEG) analysis and has been proven by many researchers to be a great tool for classification, recognition and prediction in the EEG application [1-3]. According to these research findings, it denotes a promising result in the biomedical field. Nevertheless, the use of ANN as a classifier in balancing the brainwave never has been reported via literature. However, this paper will introduce an application of ANN for the balance brainwave application. Brainwaves are grouped into four bands identified as Delta, Theta, Alpha and Beta frequency bands[4]. Delta is the lowest frequency band with the highest amplitude while Beta is the highest frequency band with the lowest amplitude. Human brain is divided into two main regions which are the right and left hemisphere. The right hemisphere is superior in thinking, remembering, perceiving, understanding and emoting whereas the left hemisphere is dominant in activities involving analysis, arithmetic, language and speech [5, 6]. Balance brainwave is using both the right and left hemisphere of brain simultaneously. Balanced thinking that simultaneously uses both right and left will lead to a balanced life and lead to better health [6, 7].

II. RELATED WORK

EEG is an example of biosignal and other biosignal are electrocardiogram (ECG), electromyogram (EMG) and magnetoencephalogram (MEG). The EEG signals are characterized by the amplitude (voltage) and frequency. The frequency varies in each band, the Delta ranges within 0.5 to 4 Hz, Theta ranges from 4 to 8 Hz, Alpha ranges from 8 to 13 Hz and Beta ranges from 13 to 32 Hz [8]. However, the raw EEG signals need to be analysed in order to extract useful information for specific research.

Generally, the EEG signals are processed using the signal processing approach which extracted based on the time and frequency. The EEG signal is collected in time based and to transform this signal into frequency based, the Fourier Transform (FT) will be employed in this signal. The EEG signal also can be processed using image processing approach via the time-frequency based. The Short Time Fourier Transform (STFT) is one of the popular techniques to process signal through time-frequency based. The STFT is to perform an FT on the signal, then mapping the signal into a two-dimensional function of frequency and time.

There are a few researches using image processing technique in biosignal. However, there is an example of using image processing technique in analysing the ECG signal. The spectrogram image was produced using STFT in order to recognize heart abnormalities in the ECG waveform [9]. Next, the spectrogram images need to be further analysed, for example by using texture analysis. Gray Level Co-occurrence Matrix (GLCM) is a popular technique in various applications such as wood, satellite and ultrasound. There is a study that uses the GLCM as a texture analysis to

detect sleep disorder breathing in the ECG signal [10]. Usually, the Principal Component Analysis (PCA) is used for data reduction, classification and regression and it has been reported elsewhere. There is a study that uses the PCA for data reduction [11]. The PCA chooses three components out of the eight components from the GLCM texture feature. The result demonstrates that the three components give better accuracy than the eight components.

ANN history begins in the year 1940's and was initiated by McCulloch and Pitts'. However, it was popular in the 1980s [12]. ANN is actually a mathematical model to solve a variety of problems in control, prediction, pattern recognition, and optimization. There are several issues in the ANN design, including the number of training samples, activation function, learning parameters, and network model and size. Nevertheless, there is no general guideline to choose the best ANN architecture for a particular size of the training. Training unconstrained networks using standard performance measures such as the mean squared error may produce an unsatisfying result [13]. ANN is highly suited to process feature rich data [12-16]. There are studies using the extracted EEG signal features to be fed into the ANN in various applications. For example, the ANN is employed to analyzed the epileptic seizure [14], Parkinson disease [15] and brain-computer interface [16].

III. EEG Spectrogram Image and GLCM Analysis

An inspiration using time-frequency based is based on research in acoustic signal [17], sound [18], heart rate from ECG [19]. There is a study using time-frequency based approach in analyzing EEG signal in Brain Computer Interface (BCI) application [16]. Based on this research, time-frequency based have the same meaning as time-frequency representation, spectrogram image and lofargram but in this paper uses the term EEG spectrogram image. In this paper, uses a STFT to generate EEG spectrogram image for balanced brain application. After produced an EEG spectrogram image, GLCM is used to extract features. GLCM is a second order texture analysis in image processing. The GLCM is used comprehensively in analyzing images texture in applications such as satellite [20], acoustic signal [17], ultrasound [21], and as well as wood recognition [22]. This paper is improvement from the previous paper [23]. The previous paper emphasizes training process in ANN, meanwhile this paper employ ANN for training and testing process. In addition, number of training to testing ratio is evaluated at 70 to 30 and 80 to 20 to find the best model. In this paper, the EEG signal is processed by using image processing technique and confirmed by the brain dominance questionnaire. Next section will be described implementing the proposed method in the experiment.

IV. Methods

A. Subjects

The data collections were performed at Biomedical Research and Development Laboratory for Human Potential, Faculty of Electrical Engineering, Universiti Teknologi MARA Malaysia. The EEG signals were collected from 51 volunteers. The volunteers comprised of 28 males and 23 females with the mean age of 21.7. All volunteers were in healthy condition and did not consume any medication prior to the test. This study was approved by the ethics committee from Universiti Teknologi MARA.

B. EEG Measurement

The EEG data were collected with 2-channel electrodes Fp1 and Fp2 and reference to earlobes A1, A2 and Fz .The electrodes using gold disc with 256Hz sampling rate and the connections are in accordance to 10-20 International system. The EEG signal was recorded for five minutes using the g.MOBIlab, with wireless EEG equipment. The setup of EEG measurement is shown in Fig. 1. The impedance was maintained below 5kΩ using Z-checker equipment. Prior to the EEG recording, volunteers have to answer the eleven items Brain Dominance Questionaire [24]. Once the questionaire is completed, the score is calculated to determine the index of each sample. This index is produced from the previous experiment [25]. Table I shows the sample per index. Index 3 is for moderately balanced brain, Index 4 is for balanced brain and Index 5 is for highly balanced brain. Data for Index 1 and Index 2, corresponding to the unbalanced brain and less balanced brain, respectively are not available.The data was collected and processed by using the MATLAB program.

Figure 1. EEG measurement set up.

TABLE I. Data sampel per index.

Index	Description	Samples
Index 3	Moderately balanced brain	9
Index 4	Balanced brain	37
Index 5	Highly balanced brain	5

C. EEG Signal Pre-processing

Fig. 2 denotes the flow diagram for the EEG signal analysis from EEG signal collection up to process classification using the ANN. EEG signal pre-processing includes the

artifact removal and band pass filter. Artifacts occur when the volunteers blink his or her eyes. This artifacts were removed by the means of a program designed using MATLAB tools by setting a threshold value. The threshold was set to eliminate data when the values are less than -100μV and more than 100μV. The band pass filter was set for the frequency from 0.5Hz to 30Hz using Hamming window with 50% overlapping.

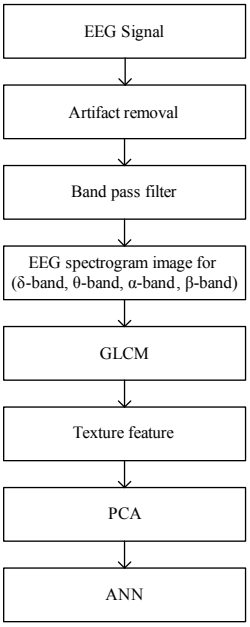

Figure 2. Flow diagram for EEG signal analysis.

D. Short Time Fourier Transform (STFT)

The STFT has produced spectrogram images for both Fp1 and Fp2 channels with image size 436 x 342. In STFT programming, each frequency band is set. The Beta band is set from 13Hz to 30Hz, Alpha band is set from 8Hz to 13Hz, Theta band is set from 4Hz to 8Hz and Delta band is set from 0.5Hz to 4Hz. The STFT is done by multiplying the Fourier Transform (FT) of the EEG signal by window function.

E. Gray Level Co-occurrence Matrix (GLCM)

There are parameters need to be set in GLCM, including the grey level, orientation and displacement. In [26] proposed grey level less than 64 and greater than 24 because grey level greater than 64 will produce an expensive computational cost whereas grey level below 24 will produce low accuracy. Most researchers employ all the four orientations (0^0, 45^0, 90^0 and 135^0) in their experiments [26, 27].The displacement, d=1 chosen by many researchers [27]. In this experiment, the grey level is set with 32, all four orientations (0^0, 45^0, 90^0 and 135^0) and displacement, d=1. Subsequently, the texture features were extracted for each GLCM. In this research, the texture feature is the combination of Haralick [27], Soh [28] and Clausi [26] technique. The 20 texture features are the Inverse difference normalized, Inverse difference moment normalized, Information of correlation 1, Information of correlation 2, Different variance, Different entropy, Sum average, Sum variance, Sum entropy, Maximum probability, Variance, Entropy, Homogeneity, Dissimilarity, Energy, Cluster prominence, Cluster shade, Autocorrelation, Contrast and Correlation.

F. Principal Component Analysis (PCA)

Output from the GLCM texture feature generates big matrices. In order to reduce big matrices, the PCA was employed to find optimum features. The optimum features will reduce the execution time for the classification process. The first principal components contain most of the useful information, and the last principal components contain mostly noise. Therefore, these last principal components can be removed without significantly affecting the information content of the GLCM texture feature.

G. Artificial Neural Network (ANN)

A feed-forward ANN was used to analysis the EEG spectrogram image and was trained using Levenberg-Marquardt algorithm [2, 14]. The system has an 8 inputs and 1 output. The best ANN model can be obtained by optimizing four parameters, namely the number of neurons in the hidden layer, epoch, momentum rate and learning rate [14] . The optimum parameters can be achieved by finding the highest accuracy and the lowest mean square error (MSE) [29]. Many studies refer to MSE as the error goal [29, 30]. In this experiment, the sigmoid was selected for the ANN activation function. The parameters to be optimized vary while the three parameters were fixed. Next, accuracy and MSE were observed and collected. Finally, the best model for the experiment was selected for the final application. This experiment uses two sets of data. The first set uses 70% of the data for training ANN and 30% of data for testing the ANN model. The second set using the ratio 80:20 for training and testing the ANN model.

V. RESULT AND DISCUSSION

Spectrogram images produced using the STFT are as shown in Figs. 3 (a)-(h). These figures illustrate the Delta band, Theta band, Alpha band and Beta band for both the Fp1 and Fp2 channels. Based on these figures, the spectrogram is texture shaped and each frequency band produces different texture. Each EEG sample will produce eight images for both channels Fp1 and Fp2. The number of spectrogram generated is shown in Table II.

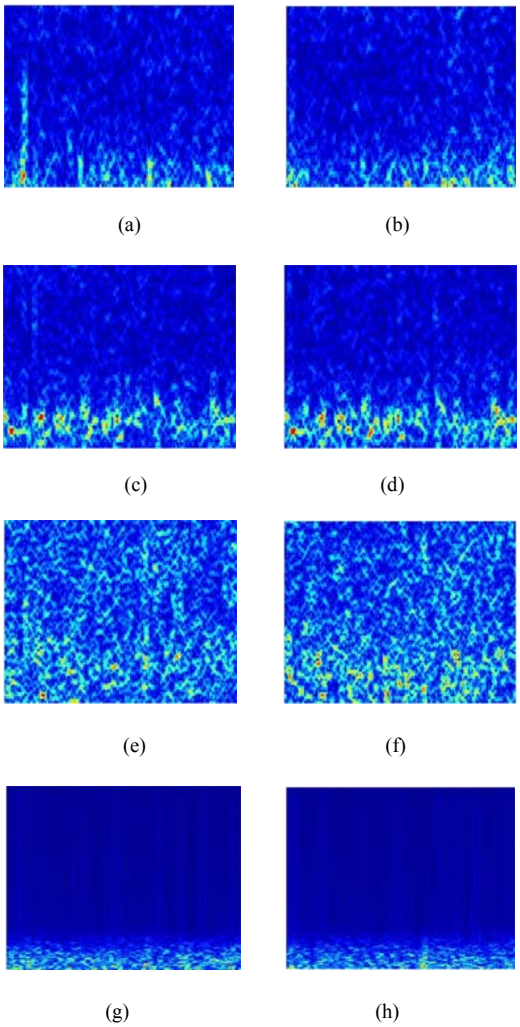

Figure 3. Spectrogram images for (a) Delta band from Fp1 channel (b) Delta band from Fp2 channel (c) Theta band from Fp1 channel (d) Theta band from Fp2 channel (e) Alpha band from Fp1 channel (f) Alpha band from Fp2 channel (g) Beta band from Fp1 channel (h) Beta band from Fp2 channel

TABLE II. NUMBER OF EEG SPECTROGRAM IMAGE.

Index	Samples	EEG spectrogram image
Index 3	9	72
Index 4	37	296
Index 5	5	40
TOTAL	51	408

The GLCM was generated for grey level=32, matrix orientations for 0^0, 45^0, 90^0 and 135^0, with displacement=1 for each spectrogram image and then texture feature from the combination of Haralick , Soh and Clausi were extracted. Eighty GLCM texture features were extracted and PCA is used to reduce this data dimension. Fig. 4 shows the percentage of eigenvalue produced by 80 principal components. The graph shows that the percentage gradually decreases until the last components. The first components show the highest percent, with 70% eigenvalue of covariance from original data. Some components have been chosen for the purpose of classification based on the results of PCA, and 8 principal components were selected because they produced a high percentage of eigenvalue.

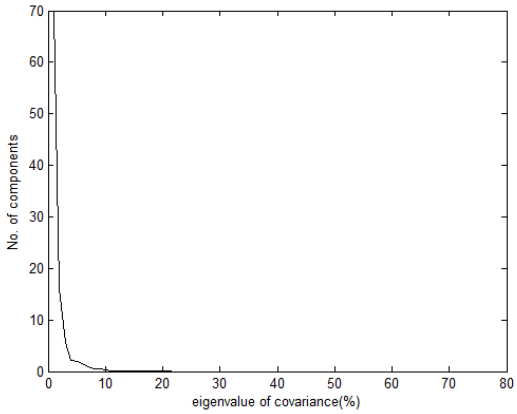

Figure 4. Graph of eigenvalue in percent

Performance of optimization of the ANN is presented in Figs. 5 to 8 for data ratio 70:30. In the figures, legend 'solid' line and 'dot' line represents mean squared error and accuracy percentage. Fig. 5 illustrates the result for optimizing the number of neurons in the hidden layer size. In the figure, the 'solid' line shows a decreasing trend with respect to the number of neurons, while the 'dot' line shows an increasing line with respect to the number of neurons. It was found that the hidden layer 24, 22, 20, 18, 13, and 10 may produce good prediction outcome. In this experiment, the network with hidden layer size 10 with accuracy rate 88.5% with MSE 0.0598 was selected.

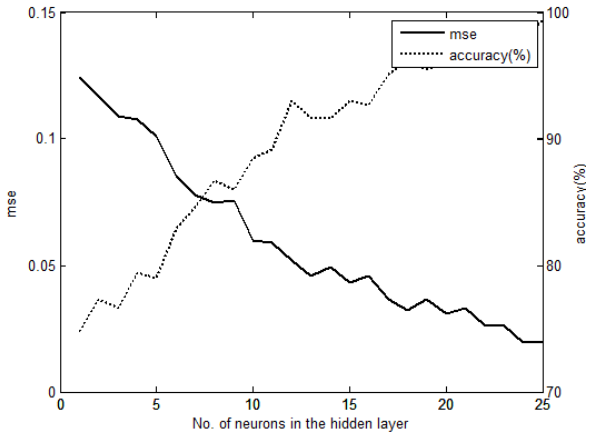

Figure 5. Training performance and prediction accuracy with varying hidden layer size

Fig. 6 shows the result of the finding of the optimum epoch. From this figure, it was found that the epoch value of 10000 and 50000 may produced good outcome. The epoch 10000 was found to be optimum with an accuracy of 88.81% with MSE 0.0937.

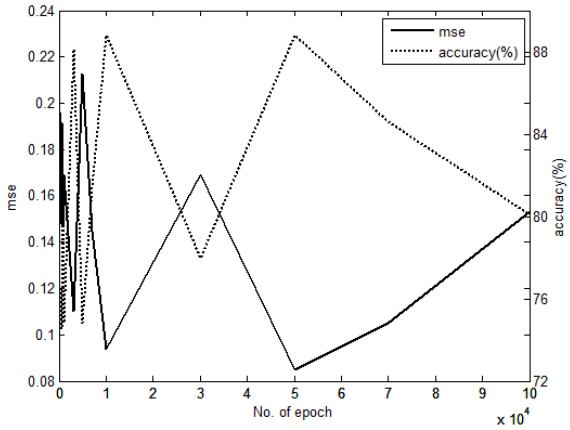

Figure 6. Training performance and prediction accuracy with varying epoch.

Fig. 7 illustrates the result of the finding of the momentum rate. From the figure, 'solid' line shows a decreasing trend until it reaches 0.3 momentum rate, at this point the trend started to increase gradually. The 'dot' line gradually decreases until it reaches 0.9 momentum rate. The figure shows a learning rate of 0.2 and 1 may produce a good prediction outcome. The momentum rate of 0.2 was found to be the optimum accuracy 89.5% with MSE 0.0586.

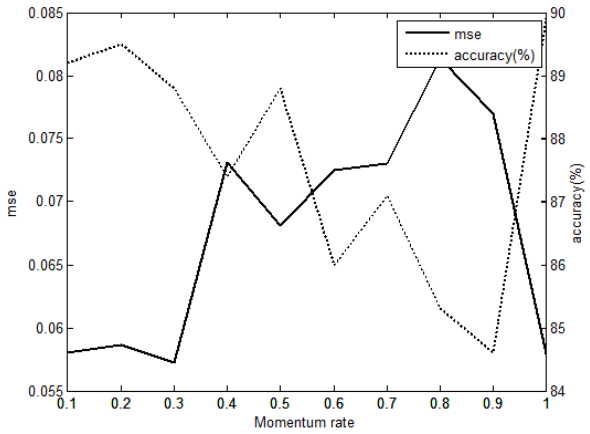

Figure 7. Training performance and prediction accuracy with varying momentum rate

Fig. 8 shows the result of the finding of the optimum learning rate. From this figure, it was found that the learning rate values of 0.2 and 0.6 may produce a good outcome with a lower point of MSE. The learning rate of 0.8 was found to be the optimum accuracy 89.2% with MSE 0.0606. Finally, the best network defined by the 10 hidden neurons, 10000 epoch, 0.2 momentum rate and learning rate of 0.6.

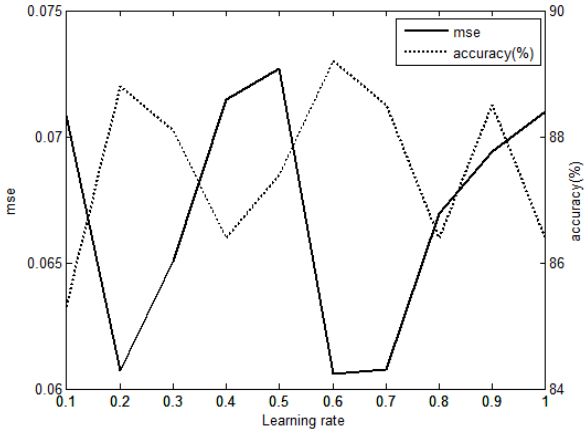

Figure 8. Training performance and prediction accuracy with varying learning rate

Table III illustrates the confusion matrix for the EEG spectrogram classification after testing using the ANN with optimized parameters. From the figure, legend I3, I4 and I5 represent Index 3, Index 4 and Index 5. From this table, accuracy for the EEG spectrogram according to the Index 3 to Index 5 is 77%.

TABLE III. CONFUSION MATRIX FOR ANN TESTING RESULT FOR DATA RATIO 70:30.

	Index 3	Index 4	Index 5
Index 3	17	6	1
Index 4	9	68	5
Index 5	0	7	9

Performance of optimization of the ANN is presented in Figs. 9 to 12 for data ratio 80:20. Again, the legend 'solid' line and 'dot' line represent the mean squared error and accuracy percentage. Fig. 9 illustrates the result for the optimizing number of neurons in the hidden layer. In the figure, it was found that the hidden layer 15, 22, 24 and 25 may produce a good prediction outcome. In the experiment, the network with hidden layer 22 with an accuracy rate of 94.21% with 0.0421 MSE was selected.

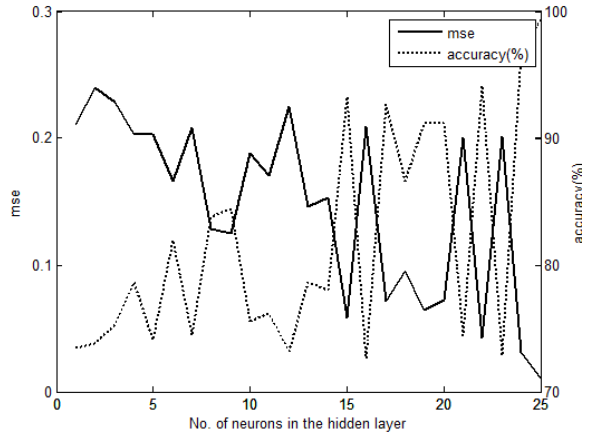

Figure 9. Training performance and prediction accuracy with varying hidden layer size

Fig. 10 shows the result for the finding optimum epoch. From this figure, it was found that epoch value of 3000, 30000 and 100000 may produce a good prediction outcome. The epoch of 3000 was found to be optimum with an accuracy of 78.5% with MSE 0.1379.

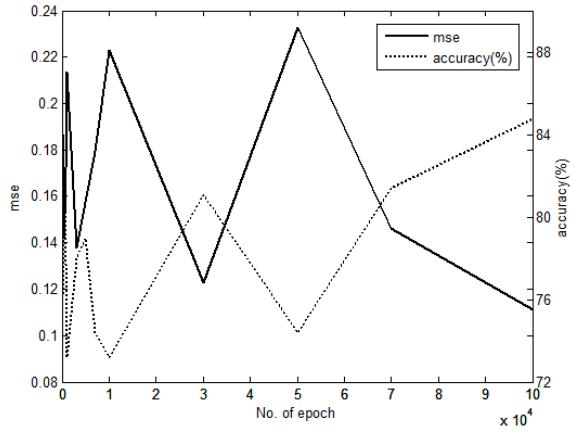

Figure 10. Training performance and prediction accuracy with varying epoch

Fig. 11 illustrates the result for the finding optimum momentum. From the figure, 'solid' line gradually decreases until reaches 0.5 momentum rates, at this point the trend started to increase. The 'dot' line reaches highest peak at point 0.5 momentum rate. In the figure shows momentum rate of 0.3 and 0.5 may produce a good prediction outcome. The momentum rate of 0.5 was found to be optimum accuracy 85.06% with MSE 0.1109.

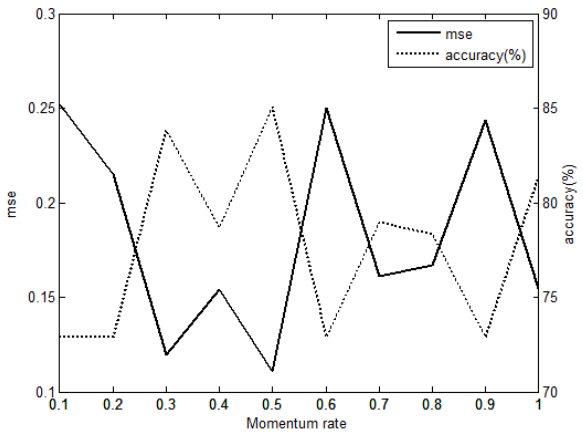

Figure 11. Training performance and prediction accuracy with varying momentum rate

Fig. 12 presents the result of finding the optimum learning rate. From the figure, it shows that the learning rates 0.6 and 0.9 may produce a good prediction outcome. The learning rate of 0.9 was found to be optimum accuracy 84.15% with MSE 0.1185. Eventually, the best network defined by 22 hidden neurons, 3000 epoch , 0.5 momentum rate and learning rate of 0.9.

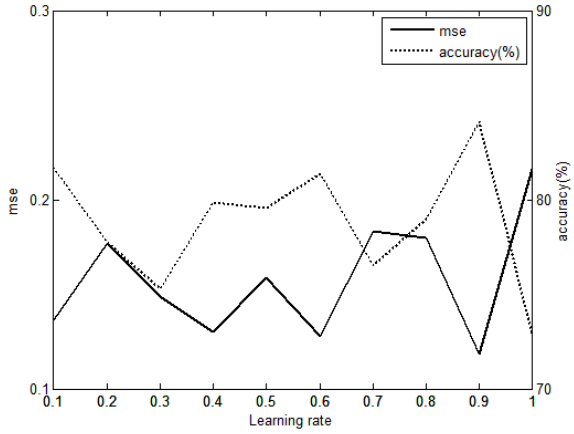

Figure 12. Training performance and prediction accuracy with varying learning rate

Table IV illustrates the confusion matrix for the EEG spectrogram classification after testing using the ANN with optimized parameters. Again, the legend I3, I4 and I5 represent Index 3, Index 4 and Index 5. From this table, the accuracy for the EEG spectrogram according to the Index 3 to Index 5 is 84%. Based on Table 2 and Table 3, the 80:20 ratio data give a higher percentage of accuracy than the

70:30 ratio data. It is therefore accepted that the training set should be larger than the testing set to obtain a higher percentage of accuracy.

TABLE IV. CONFUSION MATRIX FOR ANN TESTING RESULT FOR DATA RATIO 80:20.

	Index 3	Index 4	Index 5
Index 3	16	0	0
Index 4	4	44	8
Index 5	0	1	7

VI. CONCLUSION

In this paper, the classification using the ANN algorithm is presented with the aim to classify the EEG spectrogram as a moderate balanced brain, balanced brain and high balance brain. In order to achieve good result, the ANN model were optimized in training phase by varying the neurons in the hidden layer, epoch, momentum rate and learning rate. The accuracy rate is between 77% to 84%. The experimental result also shows that the PCA is able to reduce the original GLCM texture feature data.

ACKNOWLEDGMENT

The author would like to acknowledge the members of Biomedical Research Laboratory for Human Potential, FKE, UiTM for their support and assistance and UMP for the studentship of Mahfuzah Mustafa

REFERENCES

[1] A. Vuckovic, V. Radivojevic, A. C. N. Chen, and D. Popovic, "Automatic recognition of alertness and drowsiness from EEG by an artificial neural network," *Medical Engineering & Physics,* vol. 24, pp. 349-360, 2002.

[2] A. Subasi, A. Alkan, E. Koklukaya, and M. K. Kiymik, "Wavelet neural network classification of EEG signals by using AR model with MLE preprocessing," *Neural Networks,* vol. 18, pp. 985-997, 2005.

[3] M. K. Kiymik, M. Akin, and A. Subasi, "Automatic recognition of alertness level by using wavelet transform and artificial neural network," *Journal of Neuroscience Methods,* vol. 139, pp. 231-240, 2004.

[4] M.Teplan, "Fundamental of EEG measurement," *Measurement Science Review,* vol. 2, pp. 1-11, 2002.

[5] R. Sperry, "Left-brain, right-brain," *Saturday Review,* vol. 2, pp. 30-3, 1975.

[6] R. W. Sperry. (1981, December 8) Some Effects of Disconnecting The Cerebral Hemispheres. *Division of Biology, California Institute of Technology, Pasadena*. 1-9.

[7] P. J. Sorgi, *The 7 systems of balance: a natural prescription for healthy living in a hectic world*. Deerfield Beach, Florida: Health Communicatios, Inc., 2001.

[8] D. Cvetkovic, "Electromagnetic and audio-visual stimulation of the human brain at extremely low frequencies," PhD Thesis, RMIT University, 2005.

[9] M. Saad, M. Nor, F. Bustami, and R. Ngadiran, "Classification of Heart Abnormalities Using Artificial Neural Network," *Journal of Applied Sciences,* vol. 7, pp. 820-825, 2007.

[10] A.-A. Mohammad, B. Khosrow, J. R. Burk, E. A. Lucas, and M. Manry, "A New Method to Detect Obstructive Sleep Apnea Using Fuzzy Classification of Time-Frequency Plots of the Heart Rate Variability," in *Proceedings of the 28th IEEE EMBS Annual International Conference*, 2006, pp. 6493-6496.

[11] H. Murray, A. Lucieer, and R. Williams, "Texture-based classification of sub-Antarctic vegetation communities on Heard Island," *International Journal of Applied Earth Observation and Geoinformation,* vol. 12, pp. 138-149.

[12] A. K. Jain, M. Jianchang, and K. M. Mohiuddin, "Artificial neural networks: a tutorial," *Computer,* vol. 29, pp. 31-44, 1996.

[13] M. Egmont-Petersen, D. de Ridder, and H. Handels, "Image processing with neural networks-a review," *Pattern Recognition,* vol. 35, pp. 2279-2301, 2002.

[14] K. P. Nayak, T. K. Padmashree, S. N. Rao, and N. U. Cholayya, "Artificial Neural Network for the Analysis of Electroencephalogram," in *Proceedings of the Fourth ICISIP Fourth International Conference*, 2006, pp. 170-173.

[15] R. Rodrigues, P. Miguel, T. Teixeira, and J. Paulo, "Classification of Electroencephalogram signals using Artificial Neural Networks," in *Proceedings of the 3rd BMEI International Conference*, pp. 808-812.

[16] H. Dongmei, Z. Hongwei, and Y. Naigong, "High Resolution Time-Frequency Analysis for Event-Related Electroencephalogram," in *Proceedings of the Sixth WCICA World Congress*, 2006, pp. 9473-9476.

[17] K. S. Thyagarajan, T. Nguyen, and C. E. Persons, "An image processing approach to underwater acoustic signal classification," in *Proceedings of the IEEE Computational Cybernetics and Simulation International Conference*, 1997, pp. 4198-4203 vol.5.

[18] Y. Guoshen and J. J. Slotine, "Audio classification from time-frequency texture," in *Proceedings of the IEEE ICASSP International Conference*, 2009, pp. 1677-1680.

[19] O. H. Colak, "Preprocessing effects in time-frequency distributions and spectral analysis of heart rate variability," *Digital Signal Processing,* vol. 19, pp. 731-739, 2009.

[20] C. I. Christodoulou, S. C. Michaelides, and C. S. Pattichis, "Multifeature texture analysis for the classification of clouds in satellite imagery," *Geoscience and Remote Sensing, IEEE Transactions on,* vol. 41, pp. 2662-2668, 2003.

[21] C. I. Christodoulou, C. S. Pattichis, M. Pantziaris, and A. Nicolaides, "Texture-based classification of atherosclerotic carotid plaques," *Medical Imaging, IEEE Transactions on,* vol. 22, pp. 902-912, 2003.

[22] R. Bremananth, B. Nithya, and R. Saipriya, "Wood Species Recognition Using GLCM and Correlation," in *Proceedings of the ARTCOM International Conference*, 2009, pp. 615-619.

[23] M. Mustafa, M. N. Taib, Z. H. Murat, N. Sulaiman, and S. A. M. Aris, "The Analysis of EEG Spectrogram Image for Brainwave Balancing Application Using ANN," in *Proceedings of the 13th UKSim International Conference*, 2011, pp. 64-68.

[24] L. Mariani. (1996, 1 May 2010). *Brain-dominance questionaire*. Available: http://www.learningpaths.org/questionnaires/lrquest/lrquest.htm

[25] Z. H. Murat, M. N. Taib, S. Lias, R. S. S. A. Kadir, N. Sulaiman, and M. Mustafa, "The Conformity Between Brainwave Balancing Index (BBI) Using EEG and Psychoanalysis Test," *International Journal of Simulation Systems, Science & Technology,* vol. 11, pp. 86-92, 2010.

[26] D. A. Clausi and M. E. Jernigan, "A fast method to determine co-occurrence texture features," *Geoscience and Remote Sensing, IEEE Transactions on,* vol. 36, pp. 298-300, 1998.

[27] R. M. Haralick, K. Shanmugam, and I. H. Dinstein, "Textural Features for Image Classification," *Systems, Man and Cybernetics, IEEE Transactions on,* vol. 3, pp. 610-621, 1973.

[28] L. K. Soh and C. Tsatsoulis, "Texture analysis of SAR sea ice imagery using gray level co-occurrence matrices," *Geoscience and Remote Sensing, IEEE Transactions on,* vol. 37, pp. 780-795, 1999.

[29] N. F. Güler, E. D. Übeyli, and I. Güler, "Recurrent neural networks employing Lyapunov exponents for EEG signals classification," *Expert Systems with Applications,* vol. 29, pp. 506-514, 2005.

[30] T. Ah Chung and A. D. Back, "Locally recurrent globally feedforward networks: a critical review of architectures," *Neural Networks, IEEE Transactions on,* vol. 5, pp. 229-239, 1994.